On the Effects of Transmit Power Control on the Energy Consumption of WiFi Network Cards

Francesco Ivan Di Piazza, Stefano Mangione, and Ilenia Tinnirello

Department of Electrical, Electronic and Telecommunication Engineering (DIEET), Università di Palermo, 90128 Palermo, Italy

Abstract. Transmit power control has been largely proposed as a solution to improve the performance of packet radio systems in terms of increased throughput, spatial reuse and battery lifetime for mobile terminals. However, the benefits of transmit power control schemes on these different performance figures may strongly depend on the employed PHY technology and channel access mechanism. In this paper, we focus on the effects of power control on the energy consumption of WiFi network cards. By means of several experimental tests carried out under different operation conditions and modulation schemes, we try to justify why the reduction of the transmission power has a marginal effect on the overall energy consumption.

1 Introduction

Today, the de facto standard for wireless Internet access is the IEEE 802.11 [1] technology for Wireless Local Area Networks (WLAN), also known to the general public under the name WiFi [2]. WiFi connectivity is integrated by default in every modern portable computer, laptop and palmtop. WiFi networks for wireless Internet connectivity are available in most airports, university campuses, offices, homes, as well as in many restaurants and cafeterias. WiFi is extensively integrated in dedicated devices such as cameras, electric utilities or parking meters, and even exploited in quite specific applications such as control of garden hose sprinkles.

Due to the impressive proliferation of devices equipped with WiFi interfaces and to the limited battery power they rely on, reducing the energy consumption of WLAN interfaces is becoming a very important research issue. Indeed, several energy saving mechanisms, based on different approaches, have been recently explored in literature. Some of these mechanisms try to minimize the time intervals during which the WLAN transceiver is turned on, by means of periodic switching to a low-power doze state [3]. Although these solutions are very effective in reducing the energy consumption, they present two major drawbacks: i) they might not be applicable to ad-hoc networks, ii) they might severely degrade the quality of service in the network. The first problem arises because ad-hoc nodes have limited buffer capability. Therefore, packets destinated to a dozen node could be lost before the awekening of the node. The second problem arises because the alternating presence of sleeping nodes changes continuously the network topology

N. Bartolini et al. (Eds.): QShine/AAA-IDEA 2009, LNICST 22, pp. 463–475, 2009.

and connectivity level. In these conditions, some forms of coordination or synchronization among the nodes are required for avoiding routing problems and reducing the transport delays [4]. Moreover, common WiFi interfaces exhibit very slow transition times from a doze to an awake state, which prevent limiting the delays through high-rate switching.

Another approach to energy saving is based on the control of the transmit power. According to this approach, the transmitting node uses the minimum transmit power level that is required to communicate with the desired receiver. This mechanism reduces the power consumption of the sending node and limits the interference to other networks, thus improving both energy and bandwidth consumption. Although transmit power control (TPC) is not natively provided in WiFi networks, several research proposals [5,6,7] and emerging standards [8,9] have considered its implementation. In [6], the authors propose to extend the CTS and DATA frames in order to signal the minimum signal strength that is acceptable at the receiver and transmitter side. Similar RTS/CTS modifications are considered in [5], where a joint use of TPC and rate adaptation is proposed, so that the proper PHY rate as well as the best transmit power level can be adaptively selected. Most of these proposals [7] quantify the energy saving provided by TPC in WiFi networks via simulation. These results are based on power consumption models of WiFi interfaces, which are summarized into a set of power consumption values referring to different node states (namely, transmitting, receiving, idle and doze). Obviously, the performance evaluation of these schemes strongly depends on the setting of these values.

In this paper we deal with the problem of quantifying the energy saving that can be provided in WiFi networks by means of TPC. To this purpose, we experimentally characterize the power consumption of some commercial WiFi cards under different transmit power levels. Our methodology, similarly to the methodology described in [10,11], is able to provide: i) a direct measurement of instantaneous card consumptions, and ii) an indirect measurement of average (or per-packet) energy consumptions. Differently from previous results, we are able to rigorously control the transmit power and to compare the OFDM and DSSS modulations. Our conclusions show that little space is left to TPC for effectively reducing energy consumption of WiFi cards, due to the power consumed in idle states.

The rest of the paper is organized as follows. In section 2, we briefly review the 802.11 standard in order to define different card states corresponding to different power consumptions. In section 3, we describe our experiments, by illustrating our methodological approach and our measurement elaborations. In section 4, we try to provide a card sub-system decomposition, enlightening the fixed power consumption overheads. Finally, section 5 concludes the paper.

2 Energy Consumption in WiFi Cards

Regardless of the specific card implementation, we can expect that the energy consumption of WiFi cards depends both on physical layer (PHY) and medium

access control layer (MAC) operations. As far as concerns the PHY layer, in current 802.11a/b/g standards different modulations (e.g. DSSS and OFDM) and coding schemes are available for frame transmissions. Each scheme corresponds to a different activity interval required for transmitting or receiving a frame, which leads to different energy consumptions. Moreover, each scheme also exhibits a different processing complexity, which may cause further differences in the instantaneous power absorption. As far as concerns the MAC layer, the WiFi standard is based on a Carrier Sense Multiple Access with Collision Avoidance (CSMA/CA) protocol, called Distributed Coordination Function (DCF). DCF has been designed for optimizing wireless medium utilization while maintaining the protocol simplicity. Therefore, it is based on some design choices which do not take into account energy consumption problems. For example, the use of an asynchronous access protocol is intrinsically inefficient for the reasons discussed in this section.

DCF operations can be summarized as follows. A station with a new frame to transmit has to monitor the channel state, until it is sensed idle for a period of time equal to a Distributed InterFrame Space (DIFS). If the channel is sensed busy before the DIFS expiration, the station has to add a further backoff delay before transmitting, in order to avoid a synchronization with the transmissions of other stations. The backoff interval is slotted for efficiency reasons and is doubled (up to a maximum value) at each consecutive failed transmission. Frame transmissions have to be explicitly acknowledged with ACK frames, because the CSMA/CA does not rely on the capability of the stations to detect a collision by hearing the channel. The ACK frames are immediately transmitted at the end of a frame reception, after a period of time called Short InterFrame Space (SIFS) shorter than a DIFS. If the transmitting station does not receive the ACK within a specified ACK_Timeout, it reschedules the packet transmission, according to the given backoff rules.

These access operations imply that a new frame transmission can start at any time instants on the channel and active stations have to continuously monitor the wireless medium in order to intercept incoming frames. As a consequence, a station spends a significant amount of time in monitoring the channel, regardless of the presence of incoming or outcoming traffic. Summarizing, during the activity intervals, a WiFi card can be in various operational states, which include:

- transmission, when the card is involved in the physical irradiation of an ongoing frame;
- reception/overhear, when the card is involved in demodulating a frame destinated to itself or to another station;
- idle, when the card is monitoring the channel, ready to reveal channel busy signals, but no signal is present;
- doze, when the card radio transceiver is turned off.

Different operational states correspond to different power absorptions. Let W_{tx}, W_{rx}, W_{idle} and W_{doze} be the generic power absorbed, respectively, in transmission,

reception, idle and doze state. Regardless of the card implementation, we can expect that $W_{tx} \geq W_{rx} \geq W_{idle} \geq W_{doze}$.

Assuming that no power saving mechanism is employed (i.e. the card never switches to the doze state), the minimum energy $E_{min}(T)$ consumed in a given activity interval T is:

$$E_{min}(T) = W_{idle} \cdot T$$

This minimum consumption is experienced when the card does not transmit and receive any frames during the whole activity time. Conversely, the energy consumption is maximized when the card spends the maximum possible time in the transmission state. Since the standard limits the maximum frame size, this condition is verified when i) the card transmission buffer is never empty (i.e. the card works in saturation conditions), ii) the frames are transmitted at the minimum PHY rate, and iii) no other station accesses the channel. The ratio tx of the time spent in transmission for a card working in saturation conditions, in absence of contending stations, can be easily evaluated by considering the beginning of a new transmission as a regeneration instant. Specifically, being $\overline{b}$, T_{DATA}, and T_{ACK}, respectively, the average time spent in backoff, in transmitting a data frame and in receiving an ACK frame, it results:

$$tx = \frac{T_{DATA}}{T_{DATA} + SIFS + T_{ACK} + DIFS + \overline{b}} \tag{1}$$

For example, for the maximum admittable payload size of 2304 byte and the 802.11g PHY, it results $tx = 0.95\%$ at 6 Mbps and $tx = 0.70\%$ at 54 Mbps. The ratio rx of the time spent in reception corresponds to the ACK duration ratio within a transmission cycle, i.e.:

$$rx = \frac{T_{ACK}}{T_{DATA} + SIFS + T_{ACK} + DIFS + \overline{b}} \tag{2}$$

For example, for the previous case of 802.11g PHY with a payload length of 2304 byte and a data and acknowledgment rate of 6 Mbps, it results $rx = 1.2\%$. Given the tx ratio and rx ratio, the average power consumption $\overline{W}$ can be evaluated as:

$$\overline{W} = tx \cdot W_{tx} + rx \cdot W_{rx} + (1 - tx - rx) \cdot W_{idle} \tag{3}$$

Therefore, the energy $E(T)$ consumed during T results:

$$E(T) = \overline{W} \cdot T \leq [txW_{tx} + (1 - tx)W_{idle}] \cdot T = E_{min} + tx \cdot (W_{tx} - W_{idle}) \cdot T$$

3 Energy Consumption Measurements

3.1 Methodology

To the best of our knowledge, in literature there are a few detailed measurement studies of the energy consumption of WiFi Cards. These studies can be divided into two general approaches: i) indirect measurements, obtained by monitoring

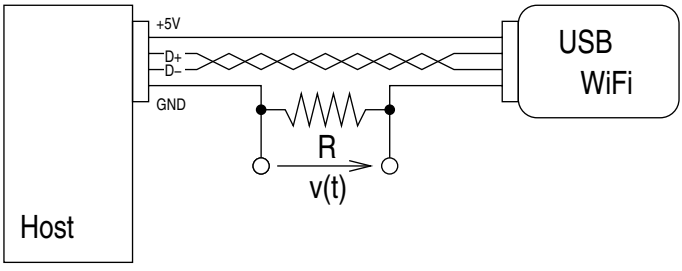

Fig. 1. Power measurement setup

the total energy consumed by laptops whose WiFi interface is enabled or disabled, ii) direct measurements, obtained by monitoring the input current drawn by the network card. We followed this second approach, for the case of USB WiFi cards. In fact, for these cards, it is immediate to probe the input current, by accessing the ground wire of the USB cable. Specifically, as shown in figure 1, we inserted a test resistor along the ground wire, in series with the card, and we measured the voltage at the resistor. Measurements were obtained using a 500 MHz Agilent digital oscilloscope, devised to acquire a complete voltage trace during an acquisition interval T. By opportunistically tuning the temporal granularity of the oscilloscope traces, we are able to monitor the current values drawn during frame transmissions, frame receptions, channel monitoring and backoff. The instantaneous power consumptions are then evaluated, in the hypothesis of fixed input voltage $V_{in} = 5V$ and resistive input impedance of the card, as:

$$P(t) = V_{in} \frac{v(t)}{R}$$

where $v(t)$ is the direct measurement of the test resistor voltage, and $v(t)/R$ is the indirect measurement of the current drawn by the card. Elaborating the oscilloscpe traces, we also averaged the instantaneous values for characterizing the W_{tx}, W_{rx} and W_{idle} values and the overall average consumption $\overline{W}$. In order to cross-validate our results, we performed some additional measurements by means of a digital multimeter. This instrument allows tracking the average power consumption at time scales much longer than a frame transmission time (e.g. 1 second). Thus, we compared these average values with the elaborations of the oscilloscope traces.

Although the results presented in this paper mainly refer to the D-Link DWL G-122 card, based on the Ralink chipset RT2500USB, we repeated our measurement campaign for other test cards (namely, Netgear WG111v2, Asus WL-167G and Linksys WUSB 300N), and for different operating systems (Windows and Linux). The host laptop was an Acer Extensa 5220, connected in ad-hoc mode with another identical laptop. As a traffic generator, we used the Iperf [12] tool with a CBR source over UDP. Unless otherwise specified, the source rate has been set to 100Mbps (in order to guarantee saturation of the transmission buffer)

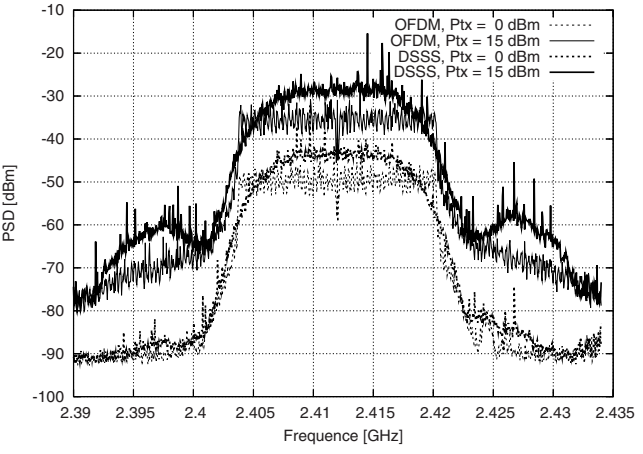

Fig. 2. Power Spectral Density of OFDM and DSSS signals, for Ptx = 15 dBm and Ptx = 0 dBm

with a frame length equal to 1470 bytes. We ran different experiments, changing the PHY transmit rate r and the PHY transmit power Ptx employed by the cards. These parameters have been changed by means of the card configuration interface at the driver level. In some cases (e.g. the very recent Linksys card), some configuration options were not available. Therefore, we used the D-Link card as a reference card thanks to the availability of a full featured driver.

We carefully checked that the values specified at the driver level were conform to the actual values adopted by the cards. About the PHY transmit rate, we considered a very simple validation test, by comparing the actual frame transmission times with the expected ones. The actual frame transmission times have been measured at the oscilloscope, by identifying time intervals during which the card drew the maximum current value. About the PHY transmit power, we monitored the RSSI values sampled at the receiver for different configuration of the transmit power, while maintaining the transmitter and the receiver node at the same position. We noticed that the RSSI values experienced increments or decrements corresponding exactly to the changes applied at the transmitter side. Some exceptions have been found when we set transmit power values higher than 15 dBm. In fact, despite the regulatory limit is higher, some cards do not allow settings higher than 15 dBm. Finally, we also checked that the power spectral density (PSD) reveled by means of a spectrum analyzer changed in agreement with the PHY transmit power. Figure 2 plots some traces of our spectrum analyzer, obtained for Ptx=15 dBm and Ptx=0 dBm, in the case of r=6 Mbps (OFDM modulation) and r=11 Mbps (DSSS modulation).

3.2 Impact of Transmit Power

Figures 3 and 4 plot the power absorption traces collected during some experiments lasting T=5 ms. The figures refer to the D-Link DWL G-122 card and

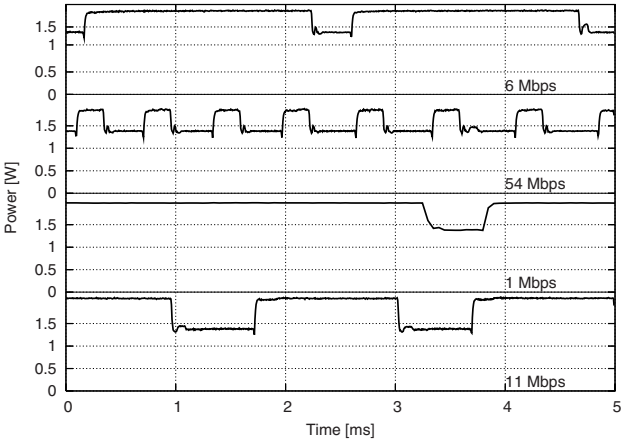

Fig. 3. Instantaneous power consumption in saturation conditions for different transmit rates - Ptx = 15 dBm

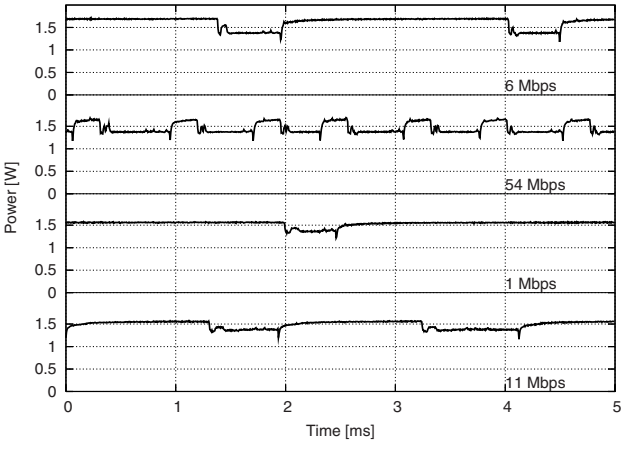

Fig. 4. Instantaneous power consumption in saturation conditions for different transmit rates - Ptx = 0 dBm

have been obtained for Ptx=15 dBm (figure 3) and Ptx=0 dBm (figure 4) at different transmit rates (namely, 1 Mbps, 6 Mbps, 11 Mbps and 54 Mbps). Unless otherwise specified, we always refer to this test card.

Focusing on figure 3, we can easily recognize the different working states of the card under test. The higher power levels correspond to the transmission states, whose duration depends on the employed rate. The time intervals between two consecutive transmissions correspond to the reception of the ACK frames and to the subsequent random backoff process. The figure visualizes that the power consumption experienced during these two phases, i.e. in reception and idle mode, is

substantially the same. In order to better visualize the ACK reception times, we set the network basic rate at 2 Mbps. In each trace, we can recognize a narrow spike over the lower level at the end of each frame transmission, which corresponds to the ACK reception. For the 54 Mbps trace, we can observe two small spikes between the transmission of the sixth and seventh frame. We verified, by means of a traffic sniffer, that this spike is due to the reception of a beacon frame transmitted by the receiver[1].

By comparing figure 3 and figure 4, it is qualitatively evident that for Ptx=0 dBm the power W_{tx} consumed in the transmission state is reduced. However, such a reduction is marginal for the OFDM modulated frames (i.e. for the 6 Mbps and 54 Mbps cases), while is appreciable for the DSSS ones. The power consumption experienced in reception and idle state is approximately the same in both the figures.

Table 1 quantifies our previous considerations. We estimated the W_{tx}, W_{rx} and W_{idle} values, by quantizing the traces plotted in figures 3 and 4 into three different levels (an high level for the transmission state, an intermediate level for the reception state, and a low level for the idle state), and by averaging the instantaneous values collected for each level. By using these estimates, we evaluated the average power consumption according to 3 and we compared such an evaluation with the trace average values and with the multimeter measurements. The average values have been summarized under the $\overline{W}$ column and identified, respectively, by the Eqn, Osc and Mul label. The results obtained with the three different methodologies are in good agreement. Since equation 3 is based on the computation of the frame transmission times, the agreement of these results also proves that the actual transmission rate is equal to the nominal one, set at the driver level.

From the table, we can observe that the power consumed in reception (W_{rx}) and idle (W_{idle}) state are comparable in all the cases. By reducing the transmit power Ptx from 15 dBm to 0 dBm, the W_{tx} values are reduced of about 20% for r=1 Mbps and r=11 Mbps (DSSS case), and about 10% for r=6 Mbps and r=54 Mbps (OFDM case). These reductions are reflected in lower percentual reduction of the average power consumption $\overline{W}$. Note that the table refers to a card working in saturation conditions. Since in most cases the transmission time is a small fraction of the whole activity time, the reduction of the W_{tx} values by means of TPC has a marginal effect on the overall energy consumption of the cards.

Finally, table 2 summarizes the results of similar measurements carried out with different cards. From the table we note that, for each card, the W_{idle} and W_{rx} values are comparable. For the cards transmitting at 15 dBm, we also note that the power W_{tx} consumed in the transmission state may vary from 1.85 W up to 2.69 W because of different card designs and implementations.

[1] We recall that in ad-hoc networks, all the nodes schedule the beacon transmission at regular time instants. When a given node succeeds in transmitting the beacon, all the other pending ones are suspended.

Table 1. Per-state and average power consumption values [W]

r	W_{tx}		W_{rx}		W_{idle}		$\overline{W}_{15dBm}$			$\overline{W}_{0dBm}$		
	15 dBm	0 dBm	15 dBm	0 dBm	15 dBm	0 dBm	Eqn	Osc	Mul	Eqn	Osc	Mul
1 Mbps	1.98	1.54	1.40	1.40	1.38	1.38	1.94	1.94	1.96	1.52	1.49	1.53
11 Mbps	2.06	1.56	1.40	1.40	1.38	1.38	1.84	1.86	1.79	1.50	1.54	1.49
6 Mbps	1.85	1.64	1.44	1.44	1.38	1.38	1.77	1.77	1.74	1.60	1.62	1.59
54 Mbps	1.85	1.64	1.44	1.44	1.38	1.38	1.57	1.55	1.51	1.49	1.46	1.44

Table 2. Power consumption values for different cards for $r = 6$ Mbps [W]

Card	Ptx	W_{tx}	W_{rx}	W_{idle}
Linksys	15	2.69	1.65	1.61
Netgear	15	2.01	1.58	1.39
Asus	12	1.40	1.01	0.97
D-Link	15	1.85	1.44	1.38

Table 3. Average power [W], average throughput [Mbps], and energy per-bit [J/b] at different rates

r	$\overline{W}$	Thr	E(T)/bit
1 Mbps	1.94	0.915	2.12e-6
11 Mbps	1.86	6.192	3.00e-7
6 Mbps	1.77	4.458	3.97e-7
54 Mbps	1.55	13.706	1.13e-7

3.3 Impact of Transmit Rate

The most evident effect of the PHY transmit rate on energy consumption is obviously related to the duration of frame transmissions. As the transmit rate increases, the ratio tx spent by the card in transmission state is reduced, thus resulting in a lower average $\overline{W}$ value. Moreover, the reduction of the transmission times allows to deliver an higher number of frames during T. Therefore, the per-bit energy consumption is further improved. Table 3 quantifies these considerations by summarizing the $\overline{W}$ (which is proportional to the energy consumption $E(T)$), the average throughput, and the per-bit energy consumption observed in saturation conditions at different rates. From the table, we can conclude that the PHY transmit rate strongly affects the per-bit energy consumption of the cards.

In section 2, we have implicitly assumed that each card is characterized by a fixed W_{tx} value, which does not depend on the transmit rate, and that such a value is constant during the whole transmission interval T_{DATA}. However, these assumptions are not rigorous. In table 1 we can see a clear difference between the OFDM and DSSS modulations (W_{tx} is about 1.8 W for the OFDM case and about 2 W for the DSSS one). While in OFDM mode the W_{tx} is about the

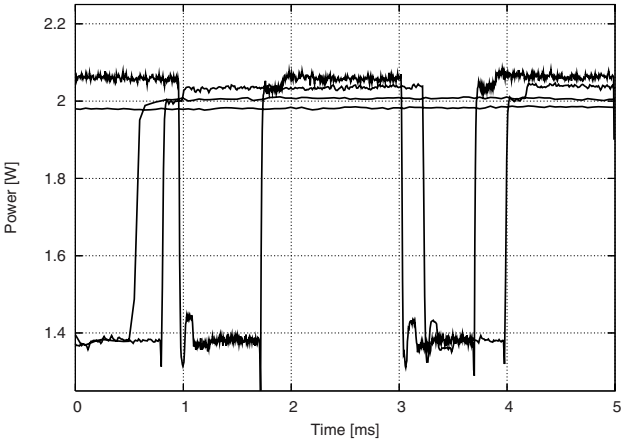

Fig. 5. Instantaneous power consumption at 1, 2, 5.5. and 11 Mbps

same for the 6 Mbps and 54 Mbps case, some differences appear in DSSS mode, as the transmit rate changes from 1 to 11 Mbps. In order to better visualize this phenomenon, figure 5 plots the instantaneous power consumption observed for the DSSS modulations. The traces collected at different rates have not been labeled, since we can easily recognize the 1, 2, 5.5 and 11 Mbps traces according to frame transmission duration.

From the figure it is evident that the instantaneous W_{tx} values slightly grow as the transmit rate increases. We suspect that this increment is due to the additional processing complexity introduced by the higher rate modulations. At the beginning of the frame transmissions, for the 5.5 Mbps and 11 Mbps traces, we can also recognize that the preamble transmission is characterized by a power consumption lower than during the rest of the frame.

4 Energy Consumption Components

The power consumption measurements described in the previous section have been obtained by considering the card under test (i.e. a D-Link DWL G-122 card) as a black box. In other words, we characterized the instantaneous power consumption without identifying the different hardware components responsible of partial absorptions. Indeed, the decomposition of the overall consumption into independent sub-systems performance can be very enlightening for the design of effective power saving schemes.

Figure 6 shows a card block diagram, analogous to the one depicted in [13]. The card has been decomposed into: a Power Amplifier (PA), an RF subsystem (RF), a MAC/BaseBand processor, and a USB host interface (USB).

Each of these sub-blocks gives a different and easily recognizable contribution to power consumption. The Power Amplifier is relevant only during transmission

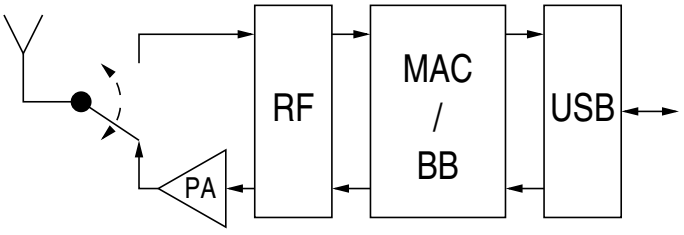

Fig. 6. System blocks of a USB WiFi card

bursts. Most WiFi implementations feature an external power amplifier. The reason for choosing an external power amplifier is that the realization of low-voltage CMOS linear power amplifiers for OFDM signals is an extremely challenging task. In fact, the OFDM signal has a very high Peak-to-Average Power Ratio (PAPR) which makes difficult designing efficient linear power amplifiers[2]. The RF subsystem, which is responsible for frequency synthesis, synchronization, up and down conversion and low-noise amplification, absorbs power while the card is not dozen. The power consumption due to baseband processing is very different depending on if the station is transmitting or receiving. When the card is in transmission state, the baseband processor just encodes and modulates the frames, thus resulting in a very lower power consumption. Conversely, when the card is in reception state, several actions are needed, such as timing and fine frequency synchronization, channel estimation and equalization and, in the case of OFDM signals, channel decoding. All these operations make the baseband processing more power-eager during reception than during transmission. Since the MAC processing has an event-based low-rate schedule, its power consumption is very low. Finally, a component which turnes out to have a significant contribution to the overall power consumption is the Universal Serial Bus interface to the host. In the following, we try to dissect separately the contribution of each component.

4.1 Power Amplifier

We can identify the power consumption W_{PA} due to the power amplifier by considering $W_{PA} = W_{tx} - W_{idle}$. From table 1, for a nominal Ptx value of 15 dBm, it results $W_{PA} \simeq 600$ mW in the case of DSSS modulations, and $W_{PA} \simeq 470$ mW in the case of OFDM modulations. Such values are compatible to a power amplifier efficiency of about 5%.

Note that the lower W_{PA} value experienced under the OFDM mode is not due to an higher efficiency in amplifying OFDM signals. In fact, by integrating the PSD traces collected by the spectrum analyzer, we found that, despite of

[2] The most efficient power amplifiers found in the literature have an efficiency which may approximately vary from 40% [14] down to less than 10% [15] as the amplifier gain increases.

the same nominal transmit power, the power radiated in OFDM mode is 4.4 dB lower that the power radiated in DSSS mode. This phenomenon can be explained as a side-effect of the non-linearity of the power amplifier. When operating in DSSS mode (i.e. with low PAPR), the power amplifier can be fed with high level signals, without triggering spectral spurs. Conversely, when operating on OFDM signals (i.e. with high PAPR), the signal levels have to be attenuated in order to avoid spur signals impairing the spectral mask requirements [2].

4.2 RF Front-End and Baseband Processing

We assume that the baseband power consumed when the card is in transmission state is neglegible. As far as concern the reception state, we identify the power consumption W_{BB} due to the baseband processing as $W_{BB} = W_{rx} - W_{idle}$. From table 1, it results $W_{BB} \simeq 20$ mW in the case of DSSS modulations, and $W_{BB} \simeq 60$ mW in the case of OFDM modulation. As expected, the W_{BB} computation leads to the same results in case of Ptx = 15 dBm and Ptx = 0 dBm.

In order to compute the RF front-end power consumption W_{RF}, we also measured the instantaneous power W_{doze} absorbed by our card while in doze state. The measurement has been carried out by switching the card transceiver off. By processing the oscilloscope traces, we obtained an average W_{doze} value of 760 mW. Assuming that W_{RF} is independent from the transmission or reception state, we consider $W_{RF} = W_{idle} - W_{doze} \simeq 620$ mW.

4.3 Universal Serial Bus/Host Interface

We assume that the power consumption resulting in the doze state is mainly due to the USB interface. Therefore, $W_{USB} \simeq W_{doze} = 760$ mW. Our measurements are compatible to the power consumption of a common USB / Host interface [13], which is about 600/700 mW. Note that this contribution represents an high fraction of the whole card consumption, being comparable to the W_{PA} value measured at full transmit power. This high value may be explained with the high speed of the PHY featured in the Universal Serial Bus specification [16].

5 Conclusions

In this paper we analyzed the power consumption of common USB WiFi cards, under different operation conditions. Specifically, we monitored the current drawn by the cards, focusing on a D-Link DWL G-122 card, for different PHY transmit rates and transmit powers. We found that reducing the transmit power has a little impact on the average energy consumption of the cards. This result, confirmed also in previous experiments [10], depends on the high power level absorbed when the card is idle, which represents a very high fixed overhead. We also found that transmit power control has a lower impact when the card works in OFDM mode rather than in DSSS mode. Finally, we tried to dissect our power consumption measurements, by identifying the consumption quota of different card subsystems, including the power amplifier, the RF-front end, the baseband and the host interface.

References

1. IEEE Standard 802.11 - 1999; Wireless LAN Medium Access Control (MAC) and Physical Layer (PHY) Specifications (November 1999)
2. Wi-Fi Alliance, http://www.wi-fi.org
3. Simunic, T., Benini, L., Glynn, P., De Micheli, G.: Dynamic Power Management for Portable Systems. In: Proc. ACM MobiCom 2000, Boston, MA, August 2000, pp. 11–19 (2000)
4. Yong, H., Ruixi, Y.: A Novel Scheduled Power Saving Mechanism for 802.11 Wireless LANs. IEEE Transactions on Mobile Computing 8(10), 1368–1383 (2009)
5. Qiao, D., Choi, S., Jain, A., Shin, K.G.: Adaptive transmit power control in IEEE 802.11a wireless LANs. In: Proc. IEEE VTC 2003, April 2003, vol. 1, pp. 433–437 (2003)
6. Agarwal, S., Katz, R.H., Krishnamurthy, S.V., Dao, S.K.: Distributed power control in ad-hoc wireless networks. In: Proc. IEEE PIMRC 2001, September 2001, vol. 2, pp. 59–66 (2001)
7. Ebert, J.P., Wolisz, A.: Combined tuning of RF power and medium access control for WLANs. Mobile Networks and Applications 5(6), 417–426 (2001)
8. Qiao, D., Choi, S.: New 802.11h mechanisms can reduce power consumption. IEEE IT Professional 8(2), 43–48 (2006)
9. Konsgen, A., Hossain, Z., Gorg, C.: Transmit Power Control Algorithms in IEEE 802.11h Based Networks. In: Proc. IEEE PIMRC 2005, September 2005, vol. 3, pp. 1441–1445 (2005)
10. Feeney, L.M., Nilsson, M.: Investigating the energy consumption of a wireless network interface in an ad hoc networking environment. In: Proc. IEEE INFOCOM 2001, April 2001, vol. 3, pp. 1548–1557 (2001)
11. Ebert, J.P., Burns, B., Wolisz, A.: A trace-based approach for determining the energy consumption of a WLAN network interface. In: European Wireless 2002, February 2002, pp. 230–236 (2002)
12. http://sourceforge.net/projects/iperf
13. Keng Fong, D., Tung, M., Lee, S., Lee, B., Wu, P., Cheng, T., Pare, J., Feng, J., Chang, E., Simpson, J., Wong, F., Jann, K., Liao, D.: A Complete Dual-band Chip-set with USB 2.0 Interface for IEEE 802.11 a/b/g WLAN applications. In: Asian Solid-State Circuits Conference 2005, November 2005, pp. 257–260 (2005)
14. Huang, C.-C., Chen, W.-T., Chen, K.-Y.: High Efficiency Linear Power Amplifier for IEEE 802.11g WLAN Applications. IEEE Microwave and Wireless Components Letters 16(9), 508–510 (2006)
15. Wang, P.-C., Huang, K.-Y., Kuo, Y.-F., Huang, M.-C., Lu, C.-H., Chen, T.-M., Chang, C.-J., Chan, K.-U., Yeh, T.-H., Wang, W.-S., Lin, Y.-H., Lee, C.-C.: A 2.4-GHz +25dBm P-1dB linear power amplifier with dynamic bias control in a 65-nm CMOS process. In: 34th European Solid-State Circuits Conference, September 2008, pp. 490–493 (2008)
16. Universal Serial Bus Revision 2.0 specification, http://www.usb.org/developers/